

LETTER • OPEN ACCESS

## The impact of COVID-19 lockdown measures on the Indian summer monsoon

To cite this article: Suvarna Fadnavis *et al* 2021 *Environ. Res. Lett.* **16** 074054



View the [article online](#) for updates and enhancements.

ENVIRONMENTAL RESEARCH  
LETTERS

## LETTER

## The impact of COVID-19 lockdown measures on the Indian summer monsoon

## OPEN ACCESS

RECEIVED  
6 September 2020REVISED  
18 June 2021ACCEPTED FOR PUBLICATION  
1 July 2021PUBLISHED  
16 July 2021Suvarna Fadnavis<sup>1,\*</sup> , T P Sabin<sup>1</sup>, Alexandru Rap<sup>2</sup>, Rolf Müller<sup>3</sup>, Anne Kubin<sup>4</sup>  and Bernd Heinold<sup>4</sup><sup>1</sup> Indian Institute of Tropical Meteorology, Ministry of Earth Sciences, Pune, India<sup>2</sup> School of Earth and Environment, University of Leeds, Leeds, United Kingdom<sup>3</sup> Forschungszentrum Jülich GmbH, IEK-7, Jülich, Germany<sup>4</sup> Leibniz-Institut für Troposphärenforschung, Leipzig, Germany

\* Author to whom any correspondence should be addressed.

E-mail: [suvarna@tropmet.res.in](mailto:suvarna@tropmet.res.in)**Keywords:** atmospheric pollution over Asia, Indian summer monsoon, impact of COVID-19 lockdownSupplementary material for this article is available [online](#)Original content from this work may be used under the terms of the [Creative Commons Attribution 4.0 licence](#).

Any further distribution of this work must maintain attribution to the author(s) and the title of the work, journal citation and DOI.

**Abstract**

Aerosol concentrations over Asia play a key role in modulating the Indian summer monsoon (ISM) rainfall. Lockdown measures imposed to prevent the spread of the COVID-19 pandemic led to substantial reductions in observed Asian aerosol loadings. Here, we use bottom-up estimates of anthropogenic emissions based on national mobility data from Google and Apple, along with simulations from the ECHAM6-HAMMOZ state-of-the-art aerosol-chemistry-climate model to investigate the impact of the reduced aerosol and gases pollution loadings on the ISM. We show that the decrease in anthropogenic emissions led to a  $4 \text{ W m}^{-2}$  increase in surface solar radiation over parts of South Asia, which resulted in a strengthening of the ISM. Simultaneously, while natural emission parameterizations are kept the same in all our simulations, the anthropogenic emission reduction led to changes in the atmospheric circulation, causing accumulation of dust over the Tibetan plateau (TP) during the pre-monsoon and monsoon seasons. This accumulated dust has intensified the warm core over the TP that reinforced the intensification of the Hadley circulation. The associated cross-equatorial moisture influx over the Indian landmass led to an enhanced amount of rainfall by 4% ( $0.2 \text{ mm d}^{-1}$ ) over the Indian landmass and 5%–15% ( $0.8\text{--}3 \text{ mm d}^{-1}$ ) over central India. These estimates may vary under the influence of large-scale coupled atmosphere–ocean oscillations (e.g. El Nino Southern Oscillation, Indian Ocean Dipole). Our study indicates that the reduced anthropogenic emissions caused by the unprecedented COVID-19 restrictions had a favourable effect on the hydrological cycle over South Asia, which has been facing water scarcity during the past decades. This emphasizes the need for stringent measures to limit future anthropogenic emissions in South Asia for protecting one of the world's most densely populated regions.

**1. Introduction**

The widespread restrictions imposed to control the rate of transmission of the Corona-Virus Disease 2019 (COVID-19) caused a drastic reduction in individual, public and freight transportation, industrial production and energy use. This resulted in substantial emission reductions of several atmospheric pollutants (Le Quéré *et al* 2020) with important regional and global impacts on air quality and climate (Forster *et al* 2020, Kanniah *et al* 2020, Le Quéré *et al* 2020).

Here, we investigate the effect of the reductions in regional atmospheric concentrations of several gases and aerosol particles on the Indian summer monsoon rainfall (ISMR) via associated changes in the atmospheric energy balance and dynamics through radiative effects (Forster *et al* 2007, Rap *et al* 2013, Fadnavis *et al* 2019a).

While COVID-19 outbreaks in the city of Wuhan, China in December 2019, it quickly spread to South Korea, Japan, Europe, and the United States during January and February 2020 (Forster *et al* 2020,

Le Quéré *et al* 2020). The first lockdown was declared in Wuhan on 23 January 2020, followed the day after by other large cities throughout the Chinese province of Hubei. Other Asian countries introduced lockdown measures during the following months: e.g. Saudi Arabia, Iran, Iraq, Kuwait, Afghanistan ([www.worldbank.org/en/region/mena/brief/coping-with-a-dual-shock-coronavirus-covid-19-and-oil-prices](http://www.worldbank.org/en/region/mena/brief/coping-with-a-dual-shock-coronavirus-covid-19-and-oil-prices)), while South Asian countries introduced such measures by the end of March (e.g. 25 March in India) ([www.mygov.in/covid-19/](http://www.mygov.in/covid-19/)). Lockdown restrictions were slowly eased after approximately two months, however with many governments still maintaining various levels of restrictions on mass gatherings, travel, and economic activities. A significant reduction (30%–40%) in aerosol loading over the Indian region during April–May 2020 compared to 2019 has been observed over the Indo-Gangetic plains by the Moderate Resolution Imaging Spectroradiometer (MODIS) during the lockdown period (Ranjan *et al* 2020). This reduction in aerosol loading has implications for the hydrological cycle.

The rapid growth of anthropogenic aerosol emissions over Asia during the last few decades played a major role in the decline of the regional hydrological cycle (Ramanathan *et al* 2005, Meehl *et al* 2008, Salzmann *et al* 2014). The aerosol loading induces an energy imbalance between the hemispheres through the aerosol direct effect, reducing the solar radiation at the surface and the land-ocean thermal contrast, which decreases the moisture inflow over the South Asian landmass. The overall effect of this increase in anthropogenic aerosol emissions on the regional hydrological cycle is a reduction in summer monsoon rainfall (Ramanathan *et al* 2005, Bollasina *et al* 2011, Ganguly *et al* 2012, Krishnan *et al* 2016, Fadnavis *et al* 2019b).

In contrast, atmospheric black carbon (BC) and dust aerosol loadings over North India (NI) and the Tibetan Plateau (TP) region during the pre-monsoon season (March to May) are known to play an important role in enhancing the ISMR (Lau and Kim 2006, Fadnavis *et al* 2017a). The dust aerosol loadings over the NI-TP region are often driven by seasonal dust transport from west Asia (Lau and Kim 2006). The desert dust loading along with local (NI) emissions of BC causes a coherent modulation of the ISMR during the monsoon season (June to September) on short time scales (i.e. weeks) (Lau 2014, Vinoj *et al* 2014, Das *et al* 2015, Dave *et al* 2017). A twofold enhancement of BC emission over India may lead to an increase in the ISMR of 1–4 mm d<sup>-1</sup> (Fadnavis *et al* 2017b).

Here, we use aerosol-chemistry climate simulations with the ECHAM6.3-HAM2.3-MOZ1.0 model (Schultz *et al* 2018, Tegen *et al* 2019) to investigate the regional radiative and dynamic effects of the reduced anthropogenic pollution levels during the COVID-19 lockdown and associated implications on

the ISMR. The reductions in anthropogenic emission due to the COVID-19 restrictions are described based on the activity decline in mobility data following Forster *et al* (2020) (see table 1 for details). Spatially varying natural emission (e.g. dust) parameterizations are kept the same in all simulations. The impact of the COVID-19 measures is eventually derived by comparing the results of the pandemic scenario (hereafter referred to as COVID-19) and the control simulation with unchanged anthropogenic emissions (referred to as CTL). We note that while particular general circulation patterns (e.g. El Niño Southern Oscillation, Atlantic Multi-decadal Oscillation, Indian Ocean Dipole) also exert a strong influence on the ISM, our methodology is designed to isolate the effect of the Asian pollution reduction during March–September caused by the COVID-19 restrictions. Indeed, 2019/2020 was characterized by a record positive phase of Indian Ocean Dipole (IOD) (Wang and Cai 2020), which would have made it difficult to clearly disentangle the COVID-19 effects. For better representability and a more independent assessment, our simulations exclusively use the meteorology of the year 2016, which was a neutral ENSO and IOD year (see supplementary section S1 available online at [stacks.iop.org/ERL/16/074054/mmedia](http://stacks.iop.org/ERL/16/074054/mmedia)).

## 2. Evaluation of model simulation

The aerosol optical depth (AOD) distribution from the control simulation (CTL) is evaluated against MODIS, and Ozone Monitoring Instrument (OMI) satellite retrievals, and Aerosol Robotic Network (AERONET) ground measurements (details in section S1). The distribution of monthly mean AOD from the model simulation and MODIS is shown in figures 1(a)–(f). Despite spatio-temporal differences, they both show a series of key common features, such as high AOD values over North India, eastern East Asia, Arabian Peninsula and Iran. During March–May, the model underestimates AOD over North India by  $\sim 0.21$  while it overestimates AOD over East Asia by  $\sim 0.28$ – $0.37$ . Over Saudi Arabia and Egypt, it overestimates AOD in March ( $\sim 0.2$ – $0.41$ ). These differences are likely due to uncertainties in the model emission inventory and transport processes (Fadnavis *et al* 2013, 2014). In addition, MODIS AOD retrievals are also known to include errors for coastal regions (Anderson *et al* 2013).

The comparison of simulated AOD (CTL) with the AERONET measurements at Kanpur and Gandhi College, in North India shows that the model underestimates AOD by 0.07–0.4 during the pre-monsoon season (figure 1(g)). However, note that the AERONET AOD anomalies of the year 2020 compared to the climatology are larger by 1.5–7.4% than the COVID-19-related anomalies in simulated AOD (COVID-19 minus CTL) at Kanpur and Gandhi College during the pre-monsoon season (figure 1(h)).

**Table 1.** National percentage changes in emissions of various species during March-May 2020 used in the COVID-19 simulation for selected Asian countries.

Aerosols/gases	March (%)	April (%)	May (%)
<b>China</b>			
BC	-13.7	-9.0	-7.6
OC	-11.3	-9.3	-7.8
CH <sub>4</sub>	-1.5	-0.2	-0.17
CO	-17.1	-13.1	-11.1
NH <sub>3</sub>	-0.51	-0.39	-0.33
NO <sub>x</sub>	-17.7	-12.3	-10.4
NMVOCs	-8.8	-6.15	-5.2
SO <sub>2</sub>	-17.6	-12.9	-10.9
<b>India, Bangladesh, Pakistan</b>			
BC	+4.8, 2.9, -2.7	-22, 8.18, -7.29	-16.8, 6.3, -4.0
OC	+4.8, +4.1, +4.2	+1.73, +13.3, +9.8	+1.8, +10.3, +7.8
CH <sub>4</sub>	+0.5, -0.7, -0.5	-2.8, -1.7, -1.9	-1.9, -1.1, -1.2
CO	+3.8, +1.8, -3.9	-20.4, +3.1, -15.4	-15, +2.6.0, -11.6
NH <sub>3</sub>	+3.8, +0.76, +0.53	+1.7, + 2.76, + 1.2	+1.40, +2.1, +1.0
NO <sub>x</sub>	+3.8, -7.9, -10.5	-40.9, -33.8, -35.3	-29.64, -24.2, -25.7
NMVOCs	+3.8, +1.3, -2.1	-13.2, +3.3, -8.7	-9.6, +2.7, -6.3
SO <sub>2</sub>	+4.8, -7.3, -7.4	-33.4, -31.9, -25.6	-23.5, -21.9, -16.8
<b>Southern countries in South Asia (average: Malaysia, Indonesia, Thailand)</b>			
BC	-10.8	-21.6	-14.4
OC	-6.28	-8.1	-6.2
CH <sub>4</sub>	-3.7	-7.1	-4.0
CO	-20.7	-29.8	-20.0
NH <sub>3</sub>	-1.7	-2.6	-1.4
NO <sub>x</sub>	-21.0	-30.7	-20.2
NMVOCs	-19.8	-20.0	-12.6
SO <sub>2</sub>	-31.1	-19.48	-13.7
<b>West Asia (average: Saudi Arabia, Iran, Iraq, Oman, United Arab Emirates)</b>			
BC	-29.35	-35	-24.1
OC	-21.6	-29.14	-23.62
CH <sub>4</sub>	-10.9	-15.7	-10.17
CO	-29.9	-39.9	-31.2
NH <sub>3</sub>	-3.7	-6.8	-5.8
NO <sub>x</sub>	-22.5	-30.0	-21.0
NMVOCs	-33.4	-26.5	-19.4
SO <sub>2</sub>	-12.9	-16.7	-12.0
<b>Japan, South Korea, Vietnam</b>			
BC	-9.4, -12.5, 0.74	-34.7, -8.9, -7.8	-31.3, -6.7, -1.9
OC	-9.7, -4.6, +2.0	-26.4, -3.3, +1.7	-25.4, -2.8, +1.4
CH <sub>4</sub>	-0.29, -2.0, -1.0	-2.0, -1.8, 0, -3.1	-1.6, -1.5, -0.97
CO	-10.8, -11.7, -6.7	-29.6, -9.2, -17.3	-30.2, -7.3, -6.0
NH <sub>3</sub>	-1.2, -1.0, +0.63	-3.6, -0.7, +0.77	-3.4, -0.53, +0.55
NO <sub>x</sub>	-9.1, -16.3, -5.9	-28.8, -12.8, -23.5	-26.7, -9.11, 8.2
NMVOCs	-4.8, -8.1, -3.8	-14.53, -6.2, -11.7	-14.3, -4.8, -3.7
SO <sub>2</sub>	-5.7, -11.1, -2.4	-23.1, 10.9, -16.7	-21.8, -9.8, -5.4
<b>Turkey</b>			
BC	-2.87	-9.71	-7.6
OC	+1.4	+4.8	+3.7
CH <sub>4</sub>	-0.67	-1.2	-0.52
CO	-1.8	-7.0	-5.5
NH <sub>3</sub>	-1.2	-3.6	-2.9
NO <sub>x</sub>	-11.8	-34.7	-24.5
NMVOCs	-1.5	-4.6	-3.10
SO <sub>2</sub>	-6.9	-17.8	-9.3

Some of these differences between simulated and observed (MODIS and AERONET) AOD are also likely caused by weather patterns which are not fully accounted for in the model.

We compare the distribution of precipitation from the CTL simulation with Global Precipitation

Climatology Project (GPCP), India Meteorology Department (IMD), and Tropical Rainfall Measuring Mission (TRMM) data (figures 1(i)–(l)) which shows a spatial variation among the different data sets. The ECHAM6-HAMMOZ model overestimates rainfall over the southern slope of the Himalayas

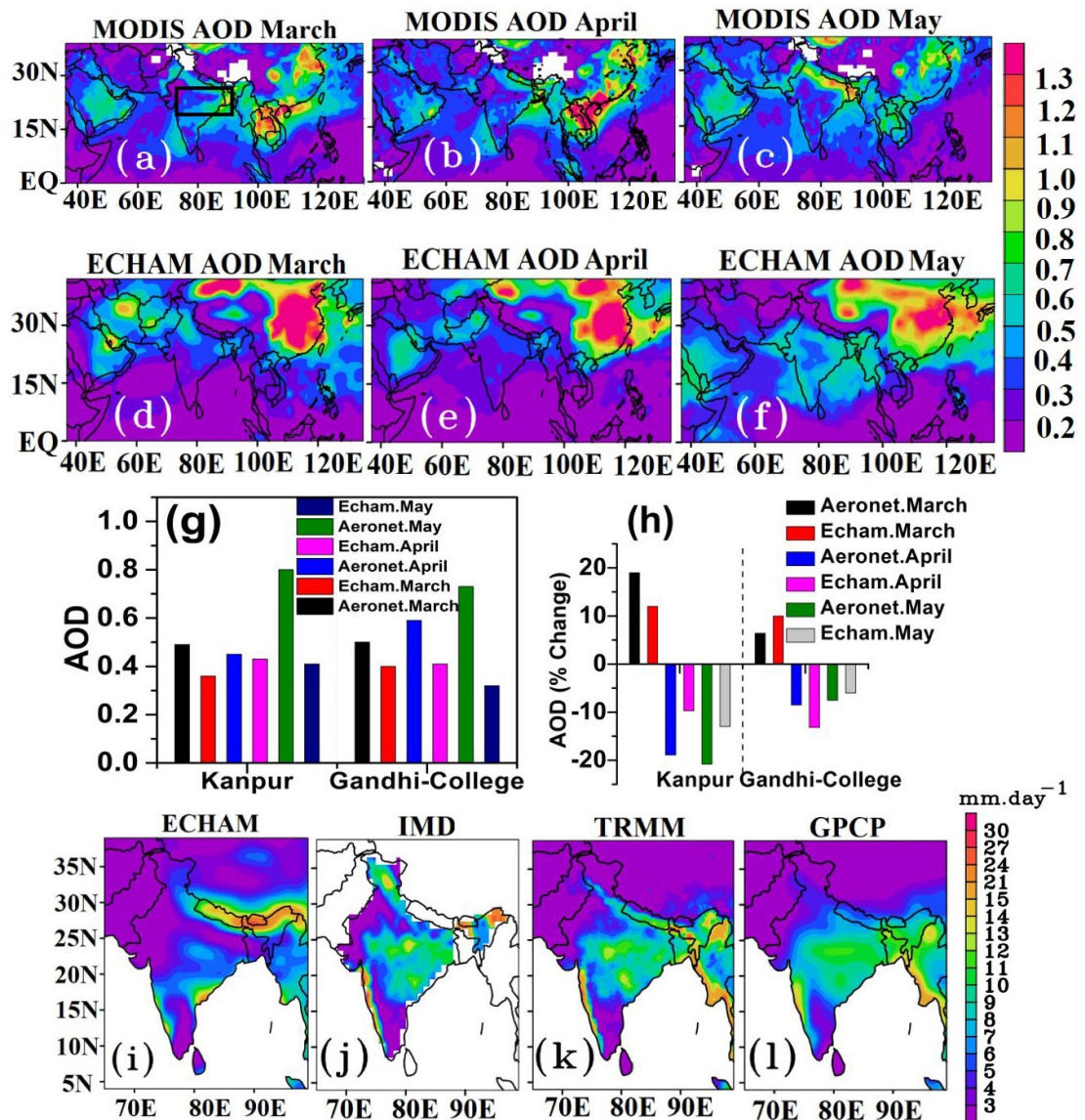


**Figure 1.** (a)–(c) Distribution of AOD from MODIS for March–May 2016, (d)–(f) same as (a)–(c) but from CTL simulation, (g) AERONET AOD at stations in North India for March–May 2016 [(Kanpur: 26.513° N, 80.232° E; and (Gandhi College: 25.871° N, 84.128° E)], (h) anomalies in AOD (%) from AERONET in March, April, and May 2020 (Kanpur climatology 2001–2019; Gandhi College climatology 2006–2019), (i) distribution of precipitation ( $\text{mm d}^{-1}$ ) from CTL simulation averaged for June to September, Observed for the year 2016 from (j) IMD rain gauge measurements (j), TRMM (k) and GPCP (l). A box in black colour in figure 1(a) indicates central India ( $78^{\circ}$ – $95^{\circ}$  E,  $18^{\circ}$ – $28^{\circ}$  N).

and underestimates over the Western Ghats. This is primarily caused by the steep orography that is not completely resolved by the model's relatively coarse resolution (Anandhi and Nanjundiah 2015). Over central India ( $78^{\circ}$ – $95^{\circ}$  E,  $18^{\circ}$ – $28^{\circ}$  N, rectangle box in figure 1(a)) the model overestimates rainfall compared to IMD and underestimates when compared to TRMM or GPCP (ECHAM:  $9.8 \text{ mm d}^{-1}$ , IMD:  $8.9 \text{ mm d}^{-1}$ , TRMM:  $11.3 \text{ mm d}^{-1}$ , GPCP:  $10.6 \text{ mm d}^{-1}$ ). There are uncertainties in the model due to transport processes, emission inventories, and various parametrizations (Fadnavis *et al* 2013, 2014, 2019b). While our model evaluation indicates certain model limitations, the fair performance of the model in simulating precipitation over India suggests that the model has sufficient skill to capture the key

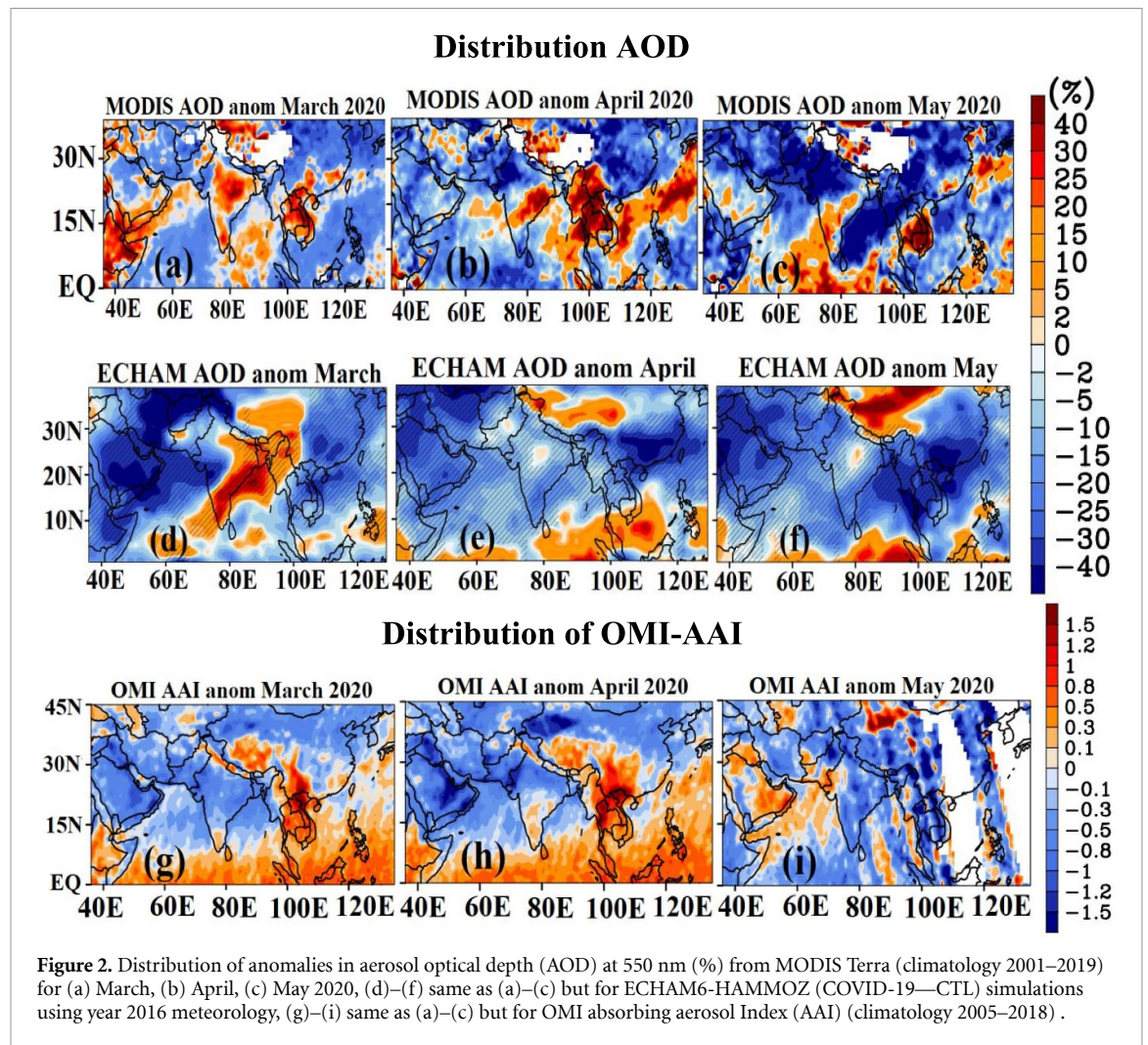
processes. Also, model bias will be less affecting the results since we are looking at the differences between the COVID-19 and CTL simulations for investigating the impact of the anthropogenic pollution reduction in ISM precipitation.

### 3. Results

#### 3.1. Reduced pollution over Asia during pre-monsoon

The evolution of the aerosol pollution during the COVID-19 lockdown period March–May 2020 is analysed in terms of AOD changes in MODIS observations and the ECHAM-HAMMOZ model results. Anomalies in MODIS AOD over the Asian





region ( $70^{\circ}$ – $135^{\circ}$  E,  $0^{\circ}$ – $45^{\circ}$  N) obtained as the difference between March and May 2020 with respect to the 2001–2019 climatology are shown in figures 2(a)–(c). The simulated AOD changes are obtained as the difference between the COVID-19 and control simulation (COVID-19 minus CTL) (figures 2(d)–(f)). Note that this comparison is only qualitative because of the differences in meteorology between 2016 used in the model and the actual year 2020. Both the MODIS and the simulated AOD indicate a  $\sim 40\%$  reduction over East Asia during March–May and over India during April–May. The  $\sim 30\%$  positive AOD anomalies over India in March are consistent with the relatively late introduction of lockdown measures in India on 25 March 2020 (at Wuhan on 23 January 2020). The AERONET measurements at Kanpur, and Gandhi College show at first positive anomalies in AOD in March 2020 (19%) but then also a reduction of  $\sim 6\%$ – $20.8\%$  in April–May (figure 1(h)). There are some spatial differences between the simulated and the MODIS observed AOD, likely due to the prevailing weather conditions. There was the unusually strong positive IOD together with the positive ENSO during 2019 (Doi *et al* 2020, Lu and Ren 2020),

which among other things, have been shown to lead to the severe 2019/2020 Australian bushfires (Harris and Lucas 2019). In addition, the very strong polar jet and the Siberian high in 2019/2020 caused the extreme heat and fires in the Siberian Arctic (Ciavarella *et al* 2020). Unlike MODIS and AERONET, the impact of such features on the AOD distribution is not picked up by the OMI absorbing aerosol index (AAI) observations which are mostly indicative of absorbing aerosols (e.g. biomass burning and dust) (figures 2(g)–(i)).

The distribution of simulated tropospheric columns of sulphate, BC, and OC aerosol show  $\sim 30\%$  reductions over South Asia in April–May (figure S1), while reductions in gaseous pollutants over South Asia in April–May vary with species, e.g. CO  $\sim 20\%$ , O<sub>3</sub>  $\sim 6\%$ , NO<sub>2</sub>  $\sim 30\%$  (figure S2). China's national network of air quality monitoring stations indicates reductions of 12% in CO and 27% in NO<sub>2</sub> during the 23 January–31 March lockdown period (Wang and Zhang 2020). This is in good agreement with our COVID-19 simulations, which show a  $\sim 10\%$  decrease in CO and  $\sim 30\%$  in NO<sub>2</sub> over China in March (figure S2).

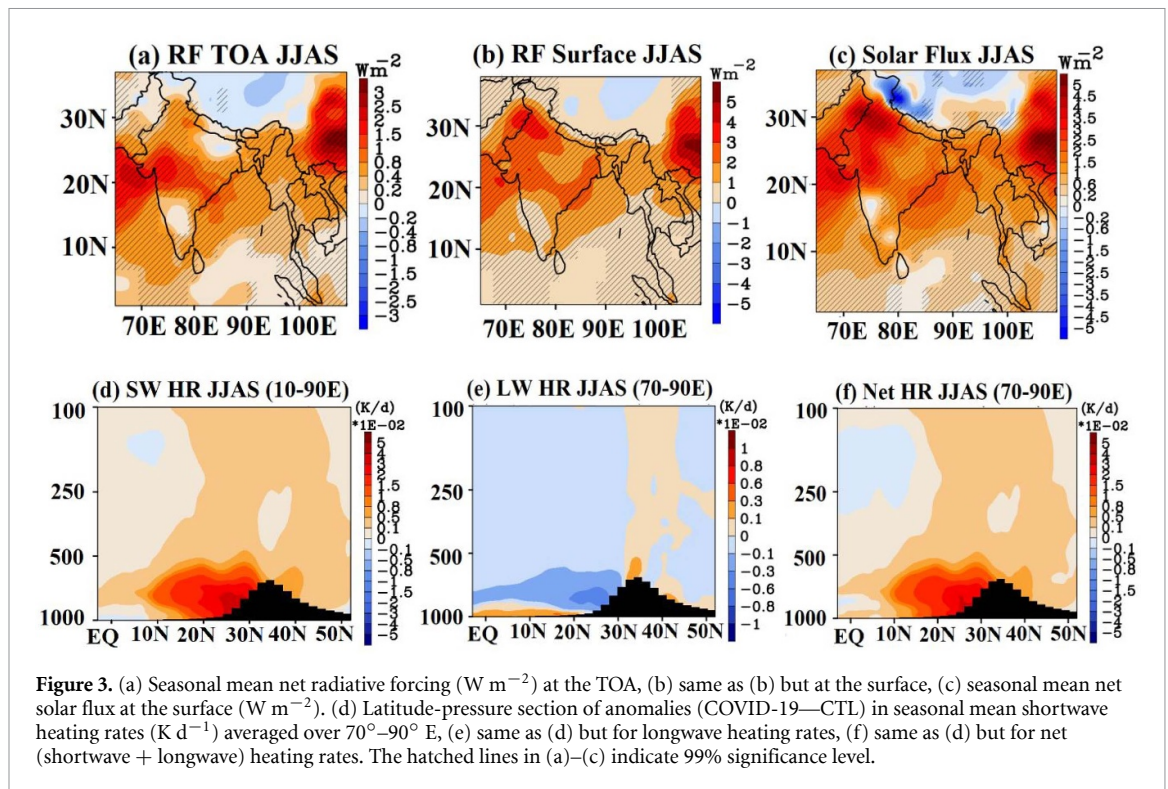


**Figure 3.** (a) Seasonal mean net radiative forcing ( $\text{W m}^{-2}$ ) at the TOA, (b) same as (b) but at the surface, (c) seasonal mean net solar flux at the surface ( $\text{W m}^{-2}$ ). (d) Latitude–pressure section of anomalies (COVID-19—CTL) in seasonal mean shortwave heating rates ( $\text{K d}^{-1}$ ) averaged over  $70^{\circ}$ – $90^{\circ}$  E, (e) same as (d) but for longwave heating rates, (f) same as (d) but for net (shortwave + longwave) heating rates. The hatched lines in (a)–(c) indicate 99% significance level.

### 3.2. Impact on radiative forcing and tropospheric heating

Changes in aerosol and gases pollution levels are known to produce changes in radiative fluxes and atmospheric heating rates due to their absorption and scattering of longwave and shortwave radiation (Ramaswamy *et al* 2009). The ECHAM6-HAMMOZ simulations (COVID-19 minus CTL) show that the impact of reduced aerosol effective radiative effects together with the radiative effects due to the changes in the atmospheric concentrations of gases led to a positive radiative forcing over central India (box in figure 1(a)) of  $0.61 \text{ W m}^{-2}$  (min:  $-0.07 \text{ W m}^{-2}$ , max:  $1.42 \text{ W m}^{-2}$ ) at TOA and  $1.69 \text{ W m}^{-2}$  (min:  $0.54 \text{ W m}^{-2}$ , max:  $3.56 \text{ W m}^{-2}$ ) at the surface (figures 3(a) and (b)) in the monsoon season. This radiative forcing is larger than the estimated  $0.37 \pm 0.26 \text{ W m}^{-2}$  produced by a doubling of Asian anthropogenic carbonaceous aerosols over the TP and Indo-Gangetic Plain during the monsoon season (Fadnavis *et al* 2017b).

Our simulations indicate that a decrease in atmospheric aerosol and gases pollution caused by the lockdown in Asia during March–April 2020 has increased the solar flux reaching the surface by  $1.6$ – $4.9 \text{ W m}^{-2}$  over the Indian landmass ( $8^{\circ}$  N– $30^{\circ}$  N) in the monsoon season. Central India shows an enhancement of  $1.65 \text{ W m}^{-2}$  (min:  $0.7$ , max:  $3.1 \text{ W m}^{-2}$ ) (figure 3(c)). In contrast, Fadnavis *et al* (2019b) showed that during the monsoon 2015 the higher than normal aerosol loading (with an increased aerosol extinction of  $33 \times 10^{-4} \text{ km}^{-1}$ ), together with co-occurring El Niño conditions,

resulted in a reduction of surface solar radiation over North India by  $5$ – $10 \text{ W m}^{-2}$ .

Figures 3(d)–(f) show anomalies in simulated shortwave, longwave, and net heating rates caused by the lockdown measures, indicating that the reduction in atmospheric pollution in 2020 increased the shortwave ( $1.5$ – $4 \times 10^{-2} \text{ K d}^{-1}$ ) and decreased the longwave ( $0.1 \times 10^{-2}$ – $0.6 \times 10^{-2} \text{ K d}^{-1}$ ) heating rates in the lower troposphere over North India ( $20^{\circ}$ – $30^{\circ}$  N), with a positive combined effect on net heating rates, in the monsoon season.

### 3.3. Implications for Asian dust transport

Another important effect of the lockdown restrictions over Asia on the ISM, in addition to reducing anthropogenic pollution, is accumulation of dust over the TP region. During the pre-monsoon (March–May) and monsoon (June–September) seasons, dust is transported in the lower and upper troposphere from western Asia to the TP region (Lau and Kim 2006, Lau *et al* 2018). This further impacts the monsoon circulation through elevated heating over the region (Lau and Kim 2006). The ECHAM6-HAMMOZ CTL experiment also shows transport of dust from western Asia to the NI and TP regions during the pre-monsoon season (figure 4(a)). The enhanced dust loading in the TP region is mostly due to the strengthening of transport from the Taklamakan desert to the TP region (figures 4(b) and S3(a)), where it accumulates during the pre-monsoon season (figure 4(c)). The distribution of zonal fluxes of dust confirms this transport from the Taklamakan desert to the TP, while the dust transport



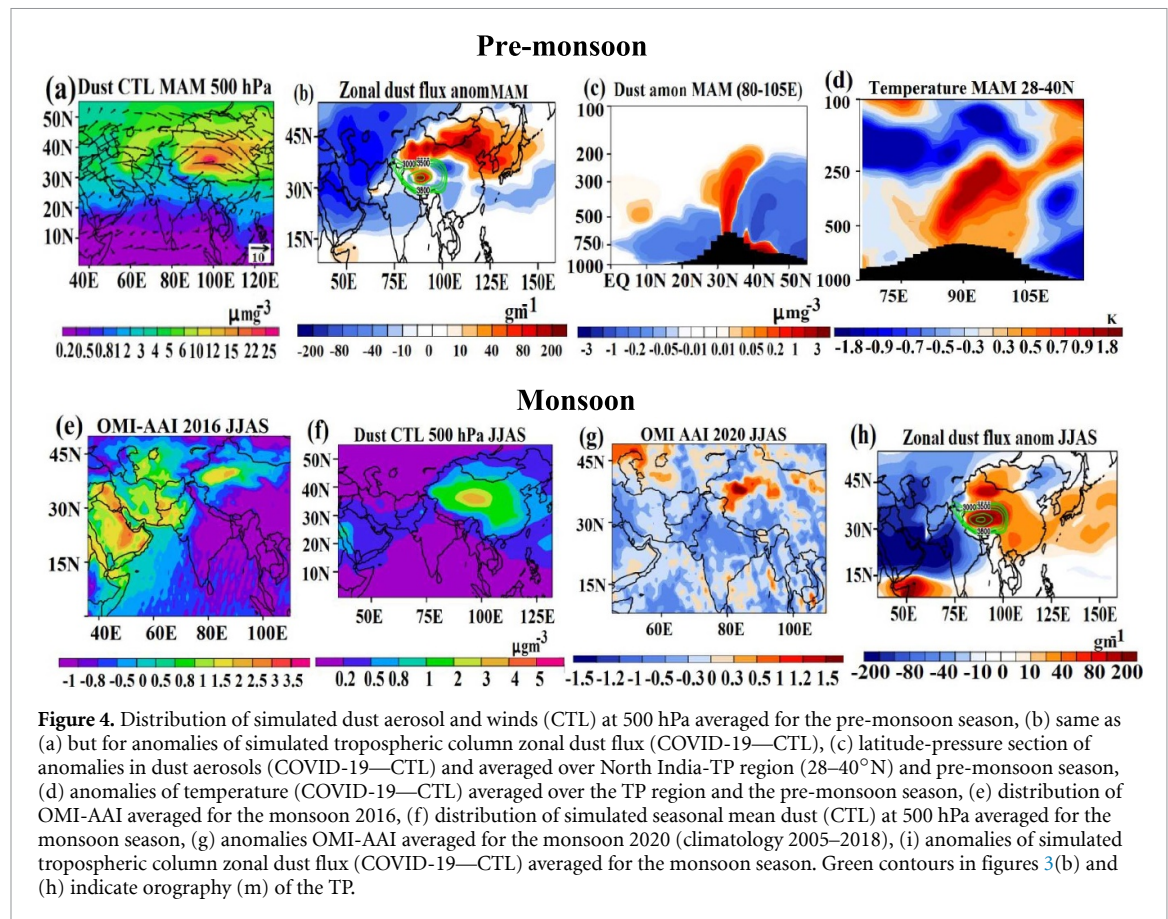


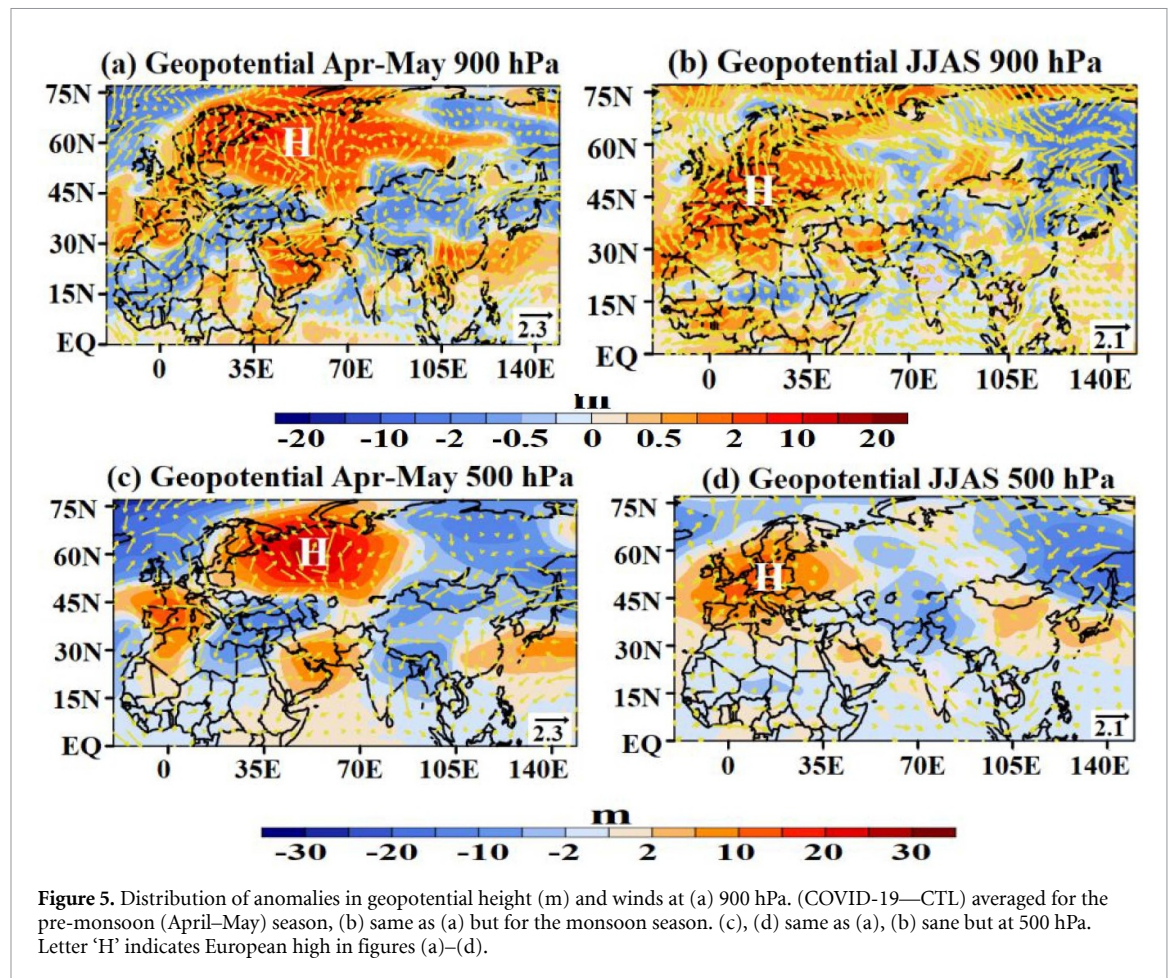
**Figure 4.** Distribution of simulated dust aerosol and winds (CTL) at 500 hPa averaged for the pre-monsoon season, (b) same as (a) but for anomalies of simulated tropospheric column zonal dust flux (COVID-19—CTL), (c) latitude-pressure section of anomalies in dust aerosols (COVID-19—CTL) and averaged over North India-TP region (28–40°N) and pre-monsoon season, (d) anomalies of temperature (COVID-19—CTL) averaged over the TP region and the pre-monsoon season, (e) distribution of OMI-AAI averaged for the monsoon 2016, (f) distribution of simulated seasonal mean dust (CTL) at 500 hPa averaged for the monsoon season, (g) anomalies OMI-AAI averaged for the monsoon 2020 (climatology 2005–2018), (i) anomalies of simulated tropospheric column zonal dust flux (COVID-19—CTL) averaged for the monsoon season. Green contours in figures 3(b) and (h) indicate orography (m) of the TP.

from western Asia is relatively less in the COVID-19 simulation (figure 4(b)). Negative anomalies of OMI AAI over western Asia in March–April 2020 also indicate that the circulation response evolved due to the lockdown restrictions lead to abating the pre-monsoon dust transport from western Asia (figures 2(g)–(i)). The OMI-AAI also shows positive anomalies over the TP in March–April 2020 compared to the 2005–2018 climatology (figures 2(i)–(g)), indicating accumulation of higher amounts of absorbing aerosols (dust) over the TP in agreement with model simulations. The accumulation of dust over the TP (COVID-19 – CTL) (figure 4(c)), generates an anomalous warming (0.5 K–1.8 K) in the NI-TP region (figure 4(d)). The tropospheric heating by dust accumulation over the TP during the pre-monsoon season leads to enhancement in the monsoon circulation according to the elevated pump hypothesis (Lau and Kim 2006).

In addition to the dust loading during the pre-monsoon season, dust accumulation during the monsoon season also shows a positive correlation with the ISMR (Lau 2014, Vinoj *et al* 2014). During the monsoon season, dust accumulation and scavenging occurs on weekly scales (Vinoj *et al* 2014). Distributions of OMI-AAI for previous monsoon seasons (e.g. 2014 and 2016) show higher AAI values in the region extending from western Asia to the TP, which may be due to transport of dust from west Asia

to the TP (figures 4(e) and S3(b)). The dust transport from west Asia during the monsoon season in the upper troposphere is also seen in the ECHAM6-HAMMOZ experiments (figure 4(f)). The distribution of OMI-AAI for the monsoon 2020 shows positive anomalies over the TP region, indicating a higher amount of dust accumulation over the TP in monsoon 2020 than in the climatology (figure 4(g)). The distribution of anomalies of simulated tropospheric column dust flux (COVID-19 minus CTL) shows higher amounts by 30–100  $\text{gm}^{-1}$  than normal over the TP (figure 4(h)). Dust is further transported from the TP to the western Pacific by the westerly winds. Thus, the lockdown effect has caused an accumulation of higher amounts of dust over the TP. The simulated effects of the lockdown measures (a combination of reduced anthropogenic aerosol and gases emissions) have altered the transport pattern of dust. Our simulations reveal that changes in dust patterns are due to amplification of the European high and a southward extension of high pressure anomalies from the European region to the Arabian Peninsula (figures 5(a)–(d)) (see section 3.4 for more details). This high pressure zone blocks the eastward transport of Saharan, Arabian and West Asian dust to the NI and TP region during the pre-monsoon (April–May) and monsoon seasons. Therefore, as can be seen in the model simulation, the seasonal mean anomalies of dust over western Asia are negative (figure S4).





Further, the stronger north-south pressure gradient due to the deepened low pressure belt over the Indian region, strengthened the dust transport from the Taklamakan desert to the TP and caused enhanced accumulation of dust there (figures 4(b) and (h)).

### 3.4. Implications on Asian summer monsoon

The changes in anthropogenic pollutants described above and the associated radiative effects also caused significant changes in the atmospheric circulation. The increase in incident solar radiation in the COVID-19 run compared to the CTL simulation resulted in a stronger surface heating and, thus, rising air motion, which led to a deepening of the anomalous low-pressure zone over the Indian subcontinent during the pre-monsoon (April–May) and monsoon seasons. On the other hand, for reasons of continuity, sinking air masses intensified the European continental high, generating a high pressure zone spanning from Eastern Europe to the Arabian Peninsula (figures 5(a)–(d) and S5(a), (b)), extending from the surface to the upper troposphere. The south-eastward extension of the European high to the Eastern Mediterranean and Middle East is associated with Rossby wave breaking (RWB) occurring in the subtropical jet (Park *et al* 2014, De Vries 2021). Anticyclonic RWB amplifies positive geopotential

anomalies (Park *et al* 2014) and their occurrence in the subtropical belt has been reported in the past (Ratnam *et al* 2012). Amplification of RWB over the European region in the COVID-19 simulation is evident in anomalies of geopotential height, temperature and distribution of potential vorticity (figures S5(a)–(h)).

Thus model results show that the COVID-19 related reductions in anthropogenic aerosol and gases pollution together with the associated enhanced accumulated TP dust increased tropospheric heating and deepening of the low-pressure zone over the Indian subcontinent during the pre-monsoon (April–May) and monsoon seasons. The absorptive radiative effects of dust led to an anomalous warming of approximately 1.5 K in the mid-upper troposphere (400–250 hPa) over North India and the TP during the pre-monsoon (figure 4(d)) and monsoon (figure 6(a)) seasons. This again contributed to further strengthening of the monsoon circulation by enhancing the cross-equatorial moisture transport towards the Indian landmass (figure S6(a)) and enhanced the ascending motion over central India (figure 6(b)). The overall effect on ISMR simulated in our model is an increase of 4% ( $0.2 \text{ mm d}^{-1}$ ) over the Indian landmass ( $70^{\circ}$ – $90^{\circ}$  E,  $10^{\circ}$ – $28^{\circ}$  N) and 5%–15% ( $0.8$ – $3 \text{ mm d}^{-1}$ ) over central India (figure 6(c)).

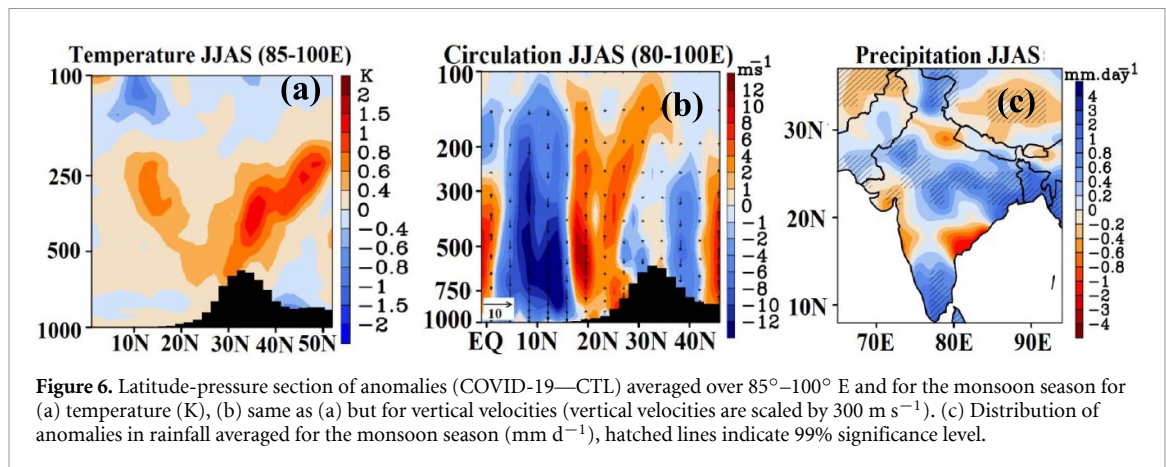


**Figure 6.** Latitude-pressure section of anomalies (COVID-19—CTL) averaged over  $85^{\circ}$ – $100^{\circ}$  E and for the monsoon season for (a) temperature (K), (b) same as (a) but for vertical velocities (vertical velocities are scaled by  $300 \text{ m s}^{-1}$ ). (c) Distribution of anomalies in rainfall averaged for the monsoon season ( $\text{mm d}^{-1}$ ), hatched lines indicate 99% significance level.

The ISMR ensemble shows a large spread in July and September but the majority of members show positive rainfall anomalies (figure S6(b)) in the monthly and seasonal timescale.

Thus, the changes in anthropogenic aerosol and gases emissions and the associated natural aerosol feedback (i.e. desert dust) caused significant changes in radiative forcing and tropospheric heating (section 3.2). The associated atmospheric circulation changes enhanced low pressure belt over the Indian region and blocking high pattern on both sides (west and east) that played an important role in amplifying a northward transport of moisture; leading to intensification of convective activity and enhancement of ISMR (Krishnan et al 2009, Priya et al 2015).

While the monsoon is known to exhibit significant intra-seasonal variability, with periods of enhanced and subdued rainfall activity (Ajayamohan and Goswami 2007, Krishnamurthy and Shukla 2007), this aspect is beyond the scope of our study. We have however further verified the monthly variations of rainfall within the monsoon season. The model does simulate monthly rainfall patterns, which are comparable with the observed patterns from IMD rain gauge measurements. The simulated monthly rainfall variabilities (figures S7(a)–(d)) are comparable with observed patterns (June–September) from the rain gauges data of India Meteorological Department (figures S7(e)–(h)) except in September, when the IMD measurements show negative anomalies of rainfall over northern India while the model shows positive anomalies. Distribution of simulated seasonal mean rainfall (figure S7(i)) also shows reasonable agreement with IMD rain gauge measurements (figure S7(j)). In the months of June, August and September, the model simulates positive rainfall anomalies over most of the Indian landmass (figures S7(a), (c) and (d)). During these months, there is a strong ascending branch over the NI-TP region ( $20^{\circ}$ – $34^{\circ}$  N) (figures S8(a), (c) and (d)), favouring the monsoon circulation, rain processes, convection (outgoing long wave radiations) (figures S8(e), (g) and (h)). Subdued rainfall in July, associated with

weak vertical motion (figure S8(b)) is further evident from the reduced outgoing long wave radiations over North India (figure S8(f)). The India Meteorological Department data show that the rainfall over the country as a whole during the second half of the season (August and September) is above-normal (96%–106%) with respect to its climatological mean. Details of intra-seasonal variations need further examination to understand the sub-seasonal role of aerosol, dust and its interaction with radiation, dynamics, and rain processes.

Our analysis shows that the direct (heating) and indirect (dust transportation) effect of the anthropogenic pollution reduction due to COVID-19 restrictions contributed to the enhanced rainfall over India via the following factors:

- The reduction in atmospheric dimming increases the surface solar radiation over South Asia and heating of the troposphere. The tropospheric heating as a result of the lowered aerosol direct effect enhances updraft over NI.
- Changes in pollution due to COVID-19 lockdown strengthen the low pressure over the Indian subcontinent and lead to the intensification and southeast-ward extension of the European continental high. The resulting strengthening of the Hadley circulation causes an enhancement of moisture inflow over the Indian landmass and an intensification of convective activity and upward motion, leading to enhancement of ISMR precipitation.
- The anomalous high pressure reduces, dust transport from western Asia while dust transport from the Taklamakan desert to NI-TP is enhanced by a stronger pressure gradient north of India during both the pre-monsoon and the monsoon season. Anomalous dust accumulation over the TP intensifies upper tropospheric warming over the NI-TP region that further intensifies the monsoon Hadley circulation and precipitation.

The intensification of ISMR is therefore the result of the combined impact of (a) the reduced aerosol direct effect over the India region and (b) the heating due to the dust aerosols over the TP.

#### 4. Summary

Results from the ECHAM6-HAMMOZ aerosol-chemistry-climate model using emissions based on national mobility data are compared with satellite observations to understand the role of reduced anthropogenic aerosol loading during the COVID-19 restrictions on the ISM. For the past 5–6 decades, India experienced a rising trend in atmospheric aerosol loading, which has been linked with a reduction in ISM precipitation and frequent droughts (Ramanathan *et al* 2005, Meehl *et al* 2008, Krishnan *et al* 2016). Lockdown measures due to the outbreak of COVID-19 have forcefully reduced aerosol pollution over the Asian region by  $\sim 40\%$ , increasing regional surface solar radiation by up to  $4 \text{ W m}^{-2}$  and tropospheric shortwave heating rates by  $0.0003\text{--}0.004 \text{ K d}^{-1}$  over India. This effect is compounded by accumulated dust over the TP region during both the pre-monsoon and the monsoon seasons leading to upper tropospheric warming ( $\sim 1.5 \text{ K}$ ) over the NI-TP region. This warming resulted in accelerated moisture inflow towards the Indian landmass and strengthened the monsoon Hadley circulation. The overall effect on seasonal mean rainfall amount is  $5\%\text{--}15\%$  ( $0.8\text{--}3 \text{ mm d}^{-1}$ ) increase over Central India. The increase in dust accumulation over the TP during the pre-monsoon and monsoon seasons in the COVID-19 compared to the control simulation is caused by dynamical changes induced by the reduction in anthropogenic emissions. These results assume that COVID-19 restrictions have not directly influenced the natural emissions (e.g. dust), and therefore natural emissions are treated (parameterised) the same in all our simulations.

It should be noted that atmospheric drivers other than anthropogenic and natural aerosols also play an important and complex role in the monsoon dynamics. While our study provides insight into the influence of emission reductions caused by COVID-19 restrictions on the ISMR, our estimates may vary under the influence of other processes (e.g. El Niño Southern Oscillation, Indian Ocean Dipole).

Our investigation further reconfirms the importance of reducing emissions of anthropogenic pollutants and its conceivable advantage in expanded water availability against the long term declining signal that India is experiencing since the middle of the last century. This will have implications for policy makers, as it indicates that reducing air pollution improves both air quality and water issues in India.

#### Data availability statement

The measurements of AOD from MODIS for March–May 2001–2020 were achieved from <https://modis.gsfc.nasa.gov/data/dataproduct/mod04.php> and Aerosol Robotic Network (AERONET) ground measurements of AOD at Kanpur ( $26.513^\circ \text{ N}$ ,  $80.232^\circ \text{ E}$ ) for 2001–2020 and Gandhi College ( $25.871^\circ \text{ N}$ ,  $84.128^\circ \text{ E}$ ) for 2006–2020 from [https://aeronet.gsfc.nasa.gov/cgi-bin/draw\\_map\\_display\\_aod\\_v3](https://aeronet.gsfc.nasa.gov/cgi-bin/draw_map_display_aod_v3). The monthly mean absorbing aerosol index from Ozone Monitoring Instrument (OMI) for March–May 2005–2020 were obtained from [www.temis.nl/airpollution/absaai/](http://www.temis.nl/airpollution/absaai/).

The rainfall data from GPCP for the period 2016 is obtained from [www.esrl.noaa.gov/psd/data/gridded/data.gpcp.html](http://www.esrl.noaa.gov/psd/data/gridded/data.gpcp.html) and TRMM\_3B42 (version 7) rainfall estimate for the period 2016 from <https://pmm.nasa.gov/data-access/downloads/trmm>. Monthly rainfall information from IMD is available at [www.imdpune.gov.in/Seasons/Pre\\_Monsoon/premonsoon.html](http://www.imdpune.gov.in/Seasons/Pre_Monsoon/premonsoon.html).

All data that support the findings of this study are included within the article (and any supplementary files).

#### Acknowledgments

The authors thank the staff of the High Power Computing Centre (HPC) in IITM, Pune, India, for providing computer resources and the team members of MODIS, AERONET, TRMM for providing data. S Fadnavis acknowledges with gratitude Professor Ravi Nanjundiah, Director IITM, Pune.

#### Author contributions

This manuscript is the combined effort of all the co-authors. S Fadnavis formulated and wrote the manuscript, with contributions from all co-authors. T P Sabin, A Rap and R Müller contributed to the analysis and presentation of the interaction of monsoon processes and aerosols, while A Rap and B Heinold contributed to the analysis of the radiative effects, atmospheric heating rates, and the temperature and pressure variation effect on dust transport. A Kubin contributed to the experiment setup and the AERONET data analysis.

#### Conflict of interest

The authors declare that they have no competing interests

#### ORCID iDs

Suvarna Fadnavis  <https://orcid.org/0000-0003-4442-0755>



Anne Kubin  <https://orcid.org/0000-0003-4120-3819>

## References

- Ajayamohan R S and Goswami B N 2007 Dependence of simulation of boreal summer tropical intraseasonal oscillations on the simulation of seasonal mean *J. Atmos. Sci.* **64** 460–78
- Anandhi A and Nanjundiah R S 2015 Performance evaluation of AR4 climate models in simulating daily precipitation over the Indian region using skill scores *Theor. Appl. Climatol.* **119** 551–66
- Anderson J C, Wang J, Zeng J, Leptoukh G, Petrenko M, Ichoku C and Hu C 2013 Long-term statistical assessment of Aqua-MODIS aerosol optical depth over coastal regions: bias characteristics and uncertainty sources *Tellus B* **65** 20805
- Berrisford P, Hoskins B J and Tyrllis E 2007 Blocking and rossby wave breaking on the dynamical tropopause in the Southern Hemisphere *J. Atmos. Sci.* **64** 2881–98
- Bollasina M A, Ming Y and Ramaswamy V 2011 Anthropogenic aerosols and the weakening of the South Asian summer monsoon *Science* **334** 502–5
- Buchard V, Da Silva A M, Colarco P R, Darmenov A, Randles C A, Govindaraju R, Torres O, Campbell J and Spurr R 2015 Using the OMI aerosol index and absorption aerosol optical depth to evaluate the NASA MERRA aerosol *Reanal. Atmos. Chem. Phys.* **15** 5743–60
- Ciavarella A et al 2020 Prolonged Siberian heat of 2020, world weather attribution (available at: [www.worldweather-attribution.org/siberian-heatwave-of-2020-almost-impossible-without-climate-change](http://www.worldweather-attribution.org/siberian-heatwave-of-2020-almost-impossible-without-climate-change))
- Das S, Dey S, Dash S K, Giuliani G and Solmon F 2015 Dust aerosol feedback on the Indian summer monsoon: sensitivity to absorption property *J. Geophys. Res. Atmos.* **120** 9642–52
- Dave P, Bhushan M and Venkataraman C 2017 Aerosols cause intra seasonal short-term suppression of Indian monsoon rainfall *Sci. Rep.* **7** 17347
- De Vries A J 2021 A global climatological perspective on the importance of Rossby wave breaking and intense moisture transport for extreme precipitation events *Weather Clim. Dynam.* **2** 129–61
- Doi T, Behera S K and Yamagata T 2020 Predictability of the super IOD event in 2019 and its link with El Niño Modoki *Geophys. Res. Lett.* **47** e2019GL086713
- Fadnavis S, Kalita G, Kumar K R, Gasparini B and Li J-L-F 2017b Potential impact of carbonaceous aerosol on the upper troposphere and lower stratosphere (UTLS) and precipitation during Asian summer monsoon in a global model simulation *Atmos. Chem. Phys.* **17** 11637–54
- Fadnavis S, Müller R, Kalita G, Rowlinson M, Rap A, Li J-L-F, Gasparini B and Laakso A 2019a The impact of recent changes in Asian anthropogenic emissions of SO<sub>2</sub> on sulfate loading in the upper troposphere and lower stratosphere and the associated radiative changes *Atmos. Chem. Phys.* **19** 9989–10008
- Fadnavis S, Roy C, Sabin T P, Ayantika D C and Ashok K 2017a Potential modulations of pre-monsoon aerosols during El Niño: impact on Indian summer monsoon *Clim. Dyn.* **49** 2279–90
- Fadnavis S, Sabin T P, Roy C, Rowlinson M, Rap A, Vernier J-P and Sioris C E 2019b Elevated aerosol layer over South Asia worsens the Indian droughts *Sci. Rep.* **9** 10268
- Fadnavis S, Schultz M G, Semeniuk K, Mahajan A S, Pozzoli L, Sonbawne S, Ghude S D, Kiefer M and Eckert E 2014 Trends in peroxyacetyl nitrate (PAN) in the upper troposphere and lower stratosphere over southern Asia during the summer monsoon season: regional impacts *Atmos. Chem. Phys.* **14** 12725–43
- Fadnavis S, Semeniuk K, Pozzoli L, Schultz G, Ghude S D, Das S and Kakatkar R 2013 Transport of aerosols into the UTLS and their impact on the Asian monsoon region as seen in a global model simulation *Atmos. Chem. Phys.* **13** 8771–86
- Forster P M et al 2020 Current and future global climate impacts resulting from COVID-19 *Nat. Clim. Change* **10** 913–19
- Forster P et al 2007 Changes in atmospheric constituents and in radiative forcing *Climate Change 2007 The Physical Science Basis* (Cambridge: Cambridge University Press) pp 131–234
- Ganguly D P, Rasch J, Wang H and Yoon J-H 2012 Climate response of the South Asian monsoon system to anthropogenic aerosols *J. Geophys. Res.* **117** D13209
- Garg A, Kankal B and Shukla P R 2011 Methane emissions in India: sub-regional and sectoral trends *Atmos. Environ.* **45** 4922–9
- Ghude S D, Kulkarni S H, Jena C, Pfister G G, Beig G, Fadnavis S and Van Der A R J 2013 Application of satellite observations for identifying regions of dominant sources of nitrogen oxides over the Indian Subcontinent *J. Geophys. Res.* **118** 1–15
- Girach I A and Nair P R 2014 Carbon monoxide over Indian region as observed by MOPITT *Atmos. Environ.* **99** 599–609
- Harris S and Lucas C 2019 Understanding the variability of Australian fire weather between 1973 and 2017 *PLoS One* **14** e0222328
- Kanniah K D, Zaman N-A-F-K, Kaskaoutis D G and Latif M T 2020 COVID-19's impact on the atmospheric environment in the Southeast Asia region *Sci. Total Environ.* **736** 1–11
- Krishnamurthy V and Shukla J 2007 Intraseasonal and seasonally persisting patterns of Indian monsoon rainfall *J. Clim.* **20** 3–20
- Krishnan R, Kumar V, Sugi M and Yoshimura J 2009 Internal feedbacks from monsoon-midlatitude interactions during droughts in the Indian summer monsoon *J. Atmos. Sci.* **66** 553–78
- Krishnan R, Sabin T P, Vellore R, Mujumdar M, Sanjay J, Goswami B N, Hourdin F, Dufresne J-L and Terray P 2016 Deciphering the desiccation trend of the South Asian monsoon hydroclimate in a warming world *Clim. Dyn.* **47** 1007–27
- Lamarque J-F et al 2010 Historical (1850–2000) gridded anthropogenic and biomass burning emissions of reactive gases and aerosols: methodology and application *Atmos. Chem. Phys.* **10** 7017–39
- Lau K-M and Kim K-M 2006 Observational relationships between aerosol and Asian monsoon rainfall, and circulation *Geophys. Res. Lett.* **33** L21810
- Lau W K M, Yuan C and Li Z 2018 Origin, maintenance and variability of the Asian tropopause aerosol layer (ATAL): the roles of monsoon dynamics *Sci. Rep.* **8** 3960
- Lau W 2014 Desert dust and monsoon rain *Nat. Geosci.* **7** 255–6
- Le Quéré C et al 2020 Temporary reduction in daily global CO<sub>2</sub> emissions during the COVID-19 forced confinement *Nat. Clim. Change* **10** 647–53
- Lu B and Ren H-L 2020 What caused the extreme Indian Ocean dipole event in 2019? *Geophys. Res. Lett.* **47** e2020GL087768
- Meehl G A, Arblaster J M and Collins W D 2008 Effects of black carbon aerosols on the Indian Monsoon *J. Clim.* **21** 2869–82
- Park T W, Deng Y and Ho C H 2014 A synoptic and dynamical characterization of wave-train and blocking cold surge over East Asia *Clim. Dyn.* **43** 753–70
- Priya P, Mujumdar M, Sabin T P, Terray P and Krishnan R 2015 Impacts of Indo-pacific sea surface temperature anomalies on the summer monsoon circulation and heavy precipitation over Northwest India–Pakistan Region during 2010 *J. Clim.* **28** 3714–30
- Ramanathan V, Chung C E, Kim D and Wild M 2005 Atmospheric brown clouds: impacts on south asian climate and hydrological cycle *Proc. Natl Acad. Sci.* **102** 5326–33
- Ramaswamy V et al 2009 Radiative forcing of climate: the historical evolution of the radiative forcing concept, the forcing agents and their quantification, and applications *Meteorol. Monogr.* **59** 14.1–14.101

- Ranjan A K, Patra A K and Gorai A K 2020 Effect of lockdown due to SARS COVID-19 on aerosol optical depth (AOD) over urban and mining regions in India *Sci. Total Environ.* **745** 141024
- Rap A, Scott C E, Spracklen D V, Bellouin N, Forster P M, Carslaw K S, Schmidt A and Mann G 2013 Natural aerosol direct and indirect radiative effects *Geophys. Res. Lett.* **40** 3297–301
- Ratnam J V, Behera S K, Masumoto Y and Yamagata T 2012 Role of rossby waves in the remote effects of the North Indian Ocean tropical disturbances *Mon. Weather Rev.* **140** 3620–33
- Sabin T P and Pauluis O M 2020 The South Asian monsoon circulation in moist isentropic coordinates *J. Clim.* **33** 5253–70
- Salzmann M, Weser H and Cherian R 2014 Robust response of Asian summer monsoon to anthropogenic aerosols in CMIP5 models *J. Geophys. Res. Atmos.* **119** 11,321–11,337
- Schultz M G et al 2018 The chemistry–climate model ECHAM6.3-HAM2.3-MOZ1.0 *Geosci. Model Dev.* **11** 1695–723
- Stevens B et al 2013 Atmospheric component of the MPI-M earth system model: ECHAM6 *J. Adv. Model. Earth Syst.* **5** 146–72
- Stier P et al 2005 The aerosol-climate model ECHAM5-HAM *Atmos. Chem. Phys.* **5** 1125–56
- Tegen I et al 2019 The global aerosol-climate model ECHAM6.3-HAM2.3—Part 1: aerosol evaluation *Geosci. Model Dev.* **12** 1643–77
- Textor C et al 2006 Analysis and quantification of the diversities of aerosol life cycles within AeroCom *Atmos. Chem. Phys.* **6** 1777–813
- Vinoj V, Rasch P J, Wang H, Yoon J-H, Ma P-L, Landu K and Singh B 2014 Short-term modulation of Indian summer monsoon rainfall by West Asian dust *Nat. Geosci.* **7** 308–13
- Wang G and Cai W 2020 Two-year consecutive concurrences of positive Indian Ocean Dipole and Central Pacific El Niño preconditioned the 2019/2020 Australian ‘black summer’ bushfires *Geosci. Lett.* **7** 19
- Wang X and Zhang R 2020 How Did Air Pollution Change during the COVID-19 Outbreak in China? *Bull. Am. Meteorol. Soc.* **101** E1645–E52
- Zhang K et al 2012 The global aerosol-climate model ECHAM-HAM, version 2: sensitivity to improvements in process representations *Atmos. Chem. Phys.* **12** 8911–49